Journal of
Data Acquisition and Processing
ISSN: 1004-9037
https://sjcjycl.cn/
DOI: 10.5281/zenodo.7735480

ANN CONTROLLER BASED SINGLE PHASE CASCADE THIRTY-ONE LEVEL GRID-TIED INVERTER FOR POWER QUALITY IMPROVEMENT

Naresh Kumar
EES, Uni. Poly. F/oEngineering & Technology, Jamia Millia Islamia, New Delhi-110025

Dr. Anwar Shahzad Siddiqui
Professor, Department of Electrical, Engineering Faculty, Jamia Millia Islamia, New Delhi-110025

Dr. Rajveer Singh
Assistant Professor, Department of Electrical, Engineering Faculty, Jamia Millia Islamia, New-Delhi-110025

Abstract: A novel multilevel inverter configuration design is presented to reduce switches and enhance waveform efficiency in a PV-Wind PowerSystem. The suggested device operates under binary asymmetric circumstances to create a high output voltage level with little harmonic distortion. One unipolar sinusoidal reference with fifteen carriers is utilized to generate the requisite switching pulses and provide the appropriate output voltage level. For creating the 31-level output voltage level with a total harmonic distortion (THD) value that matches the harmonic norm of IEEE 519, the suggested arrangement requires eight unipolar switches. A digital multi carrier PWM method with PI, Fuzzy, and ANN controllers is constructed in a MATLAB simulation, and the suggested system is evaluated using an experimental configuration utilizing the DSPIC30F2010 Controller.

Keywords—PV-Wind Power System, flyback converter, (ASCHBMLI) asymmetrical cascaded H Bridge multi-level inverter, DSPIC30F2010

I. INTRODUCTION

These topologies are referred to be asymmetrical topologies since the total of output voltage level is to be created in ASCHBMLI in addition to estimatevoltage sources (DC) to be determinedfor binary. In binary proportions, the greatest voltage level at the outputcan be given by using,[2{1 + 2 + 4 + 8} +1] = 31. The ASCHBMLI inverter receives electricity from the SPV and wind system using DC-DC flyback converter. The SPV is connected oninput of this flyback mechanismand the fuzzy interface-based controller is suggested to achieve enhanced control for it. The converter's secondary is controlled by selecting appropriate voltages (6V,12V,24V and 48V) compared to the traditional PI controller.

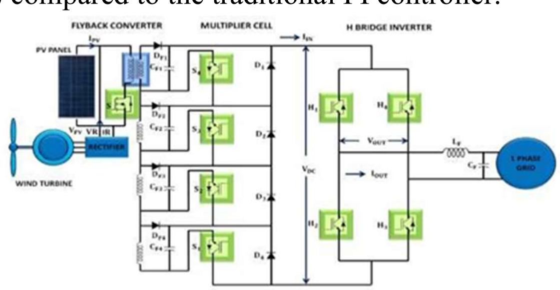

Fig. 1. 31-level ASCHBMLI block diagram

The flyback converter's output is linked to the 31 ASCHBMLI. The output of the ANN controllerused to integrate the frequency and grid voltage is superior to that of Fuzzy and standard PI controllers. This article investigates and simulates a PV-wind hybrid generating system with a grid that includes a an inverter and converter. Finally, the suggested device Microcontroller DSPIC30F2010 is tested with a prototype in order to verify the converter and inverter output.

II. PROPOSED FLY BACK CONVERTER WITH MPPT TECHNIQUES

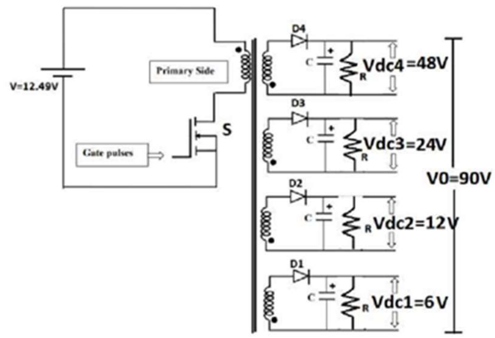

Fig.2. Block diagram of proposed flyback converter

First During operation, the fly-back converter assumes several Circuit configurations. Circuit operating modes are the names given to each of these circuit setups. The whole operation of the power supply circuit is clarified with the use of real similar circuits in these distinct states. The transformer's primary winding is linked to the input, and switch 'S' is on supply, with its dotted end hooked to the beneficial hand. The diode 'D' connected in series with the secondary winding is reverse biased at this moment due to the induced voltage in the secondary. As a result, when switch 'S' is turned on, the main winding may hold current, but current is stopped in the secondary sidebecause of reverse biased diode. The main winding current is fully responsible for the flux creation in the center of the transformer and the relationship between the windings.

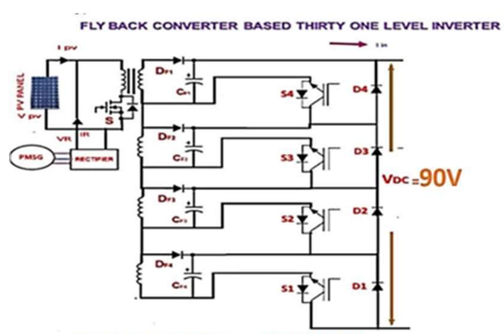

Fig 3. Fly-back converter based 31-level asymmetrical multi-level inverter

In continuous current mode, the operation is analyzed in two modes:

A. Mode I (Switch S is ON)

The switch is kept in ON position for the interval, where k is duty cycle, T is period of switching. The voltage across and current through the inductance (primary winding) is Vp and

Ip. As the voltage present at secondary winding in opposite polarity, diode DF1 reverse biased and load gets disconnected from the source but the capacitor gives supply to load shown in fig.3(a) and 3(b) .

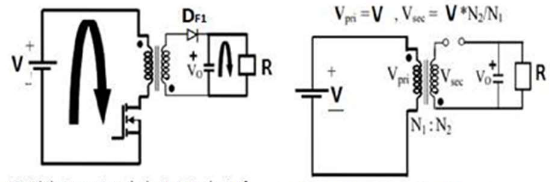

Fig.3(a): Current path during Mode-1 of circuit operation

Fig.3(b): Equivalent circuit in Mode-1

The relation between voltage and current in inductance is given by:

$$I_p = \frac{V_p}{L_p} t \quad (1)$$

At timet, the current reaches its maximum value as given below:

$$I_{p(peak)} = \frac{V_p}{L_p} kT \quad (2)$$

The current through the secondary winding is

$$I_{s(peak)} = \frac{N_p}{N_s} I_{p(peak)} \quad (3)$$

The relation between source voltage and primary winding current is

$$V_{pv} = L_p \frac{d}{dt} I_p \quad (4)$$

Let the capacitor be in full charge in this mode, hence the voltage at secondary side will be constant

$$V_s = \frac{N_p}{N_s} V_{pv} \quad (5)$$

The energy stored in this mode is given by

$$\text{Energy} = \frac{1}{2} L_p I_p^2 \quad (6)$$

The load(R) will get continuous current as the capacitor is already stored with charge. B. Mode II (Switch S is OFF)

The switch has now been turned off. In figs. 3(c) and 3(d), the reversal of winding polarity does not change the current direction in the primary winding, which turns on the diode DF1, charges the capacitor, and delivers current to the next step.

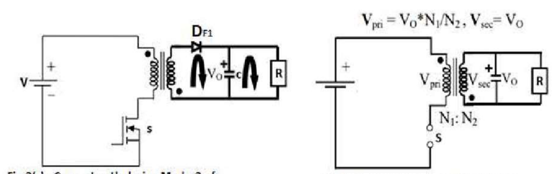

Fig:3(c) : Current path during Mode-2 of circuit operation

Fig.3(d): Equivalent circuit in Mode-2

The decrease in secondary winding current is expressed as

$$I_s = I_{s\ peak} - \frac{V_O}{L} t \quad (7)$$

The input power is expressed as

$$P_i = \frac{1}{2} L_p I_{p(peak)}^2 = \frac{(kv_p)^2}{2fL_p} \quad (8)$$

The output power is given by

$$P_o = \eta P_i = \eta \frac{(kv_p)^2}{2fL_p} = \frac{v_0^2}{R} \quad (9)$$

From the above expression, the output voltage is given by $v_o = v_p k \sqrt{\frac{\eta R}{2fL_p}}$ (10)

C. PI controller based MPPT

The u(t) output signal is proportional to both the VI(t) input signal and the VI(t) input signal integral, and is determined by the VI(t) input signal.

$$u(t) = K_p v_i(t) + K_i \int v_i(t)dt \quad \text{----------- (11)}$$

Figures 4(a) and 4(b) illustrate a Simulink schematic of a fly-back converter using an analogue PI controller (b).

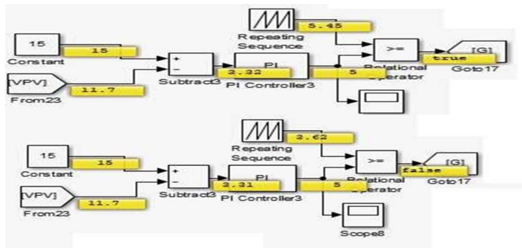

Fig. 4(a) and (b). simulation diagram for MPPT with pi controller

In the PI controller, there are two parameters: KP and KI. This MPPT has a Vref=15V reference voltage. This Vref=15 is compared to the PV-Wind voltage (Vpv-wind) and an error signal is generated, which is processed to produce a control voltage via the PI controller and gives an output from 0 to 1 corresponding to 0% and 100% duty cycle by correctly selecting Ki=100 and Kp=100 values (although typically it is limited to 5), a repeating sequence of time values [0 1], and a repeating sequence of time values [0 1]. This creates a saw tooth, which is then compared to a number between 0 and 1. The control voltage is fed into the PWM generator, which controls the DC switch and the frequency at fs=1000Hz. Once the PV-Wind power is fed into the flyback converter and the PI controller is turned on, the duty cycle value varies, changing the input value sensed by the PI controller.

D. Fuzzy logic based MPPT controller

Table 2 Performance Factors

Figure 5 shows a block diagram of a fuzzy logic controller (FLC). Fuzzification, defuzzification, and an inference engine which are then handed to the defuzzifier to generate the control voltage utilised to input the switch control to the PWM generator.

Table-1 Rules for FLC

	CHANGE IN ERROR							
		NL	NM	NS	ZE	PS	PM	PL
ERROR	NL	NL	NL	NL	NL	NM	NS	ZE
	NM	NL	NL	NL	NM	NS	ZE	PS
	NS	NL	NL	NM	NS	ZE	PS	PM
	ZE	NL	NM	NS	ZE	PS	PM	PL
	PS	NM	NS	ZE	PS	PM	PL	PL
	PM	NS	ZE	PS	PM	PL	PL	PL
	PL	ZE	PS	PM	PL	PL	PL	PL

In the FLC, there are two parameters: error E and change in error E. This MPPT has a Vref=15V reference voltage. This Vref=15 creates an error signal that is processed via the FLC to produce a control voltage and to better compare error and change in error E adjustments when compared to the PV-Wind voltage (Vpv-wind). This voltage control value compares the saw tooth's reference value and generates a pwm pulse to turn on and off the mosfet switch illustrated in the simulation diagram below.

Table 1 shows the rules given to the fuzzifier for the inference engine's processing of the membership functions

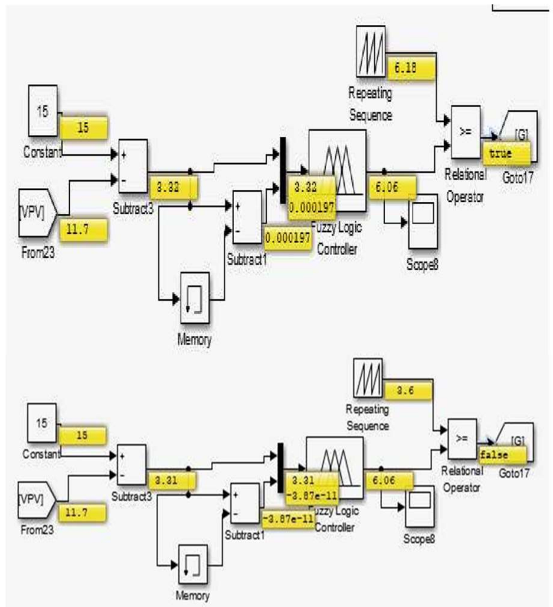

Fig. 6(a) and (b). simulation diagram for MPPT with pi controller

To achieve increased control for DC-DC converters, a fuzzy logic controller-based controller is suggested, as shown in table 2 below, when compared to typical PI controllers and performance parameters comparison.

III. PROPOSED 31-LEVEL ASCHBMLI

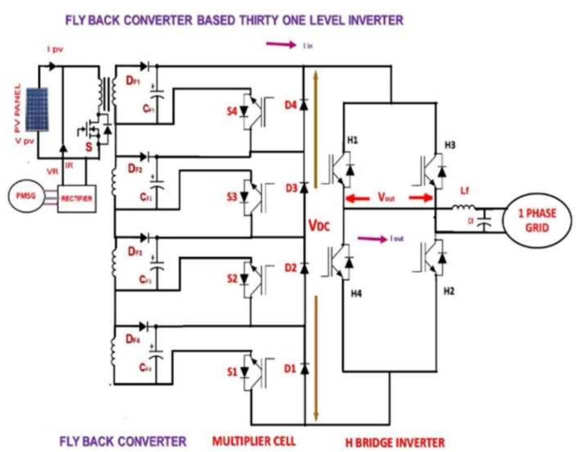

Fig..7 block diagram for Single-Phase 31 level ASCHBMLI

A 31-Level ASCHBMLI is depicted in Figure 7. ASCHBMLI consists of eight IGBTs and four diodes. Input voltages Vdc1=6V, Vdc1=12V, Vdc1=24V, and Vdc1=48V. The voltages at the output of ASMLIare 6, 12, 18, 24, 30, 36, 42, 48,54, 60, 66, 72, 78, 84, 90,0, -6, -12, -18, -24, -30, -36, -42, -48, -54, -60, -66, -72, -78, -84 and -90 voltsthat is 31-levels.Switching pulse at the gate is achieved by a sinusoidal signal& by DC-offset voltage. Both of these signals can be compared by AND & OR relational operators to generate a gate pulse. In a positive cycle, the H-bridge inverter's switches H1, H2 are turned on while H3, H4 are turned off. H1 and H2 are turned off during the negative cycle, while H3, H4 are turned on, as seen in table 3. To regulate the inverter at first, a basic multicarrier modulation approach was used. At a reduced switch inverter arrangement, the activating pulses are achieved by the PWM technique of unipolar multicarrier phase disposition (UPD). Bipolar techniques are commonly utilized to generate pulses for inverter switches. Unipolar PWM has the advantage of halving the need for a carrier signal as compared to Bipolar PWM. In the unipolar approach '(L-1)/2,' carriers are employed to generate 'L' output voltage levels. Phase Disposition is a type of level shifting PWM method (PD).

TABLE 3. SHOWS THE SWITCHING TABLE

Modes	Conducting switches and diodes	Output voltage	Modes	Conducting switches and diodes	Output Voltage
1	S_1, D_2, D_3, D_4, H1,H2	6V	1	S_1, D_2, D_3, D_4, H3,H4	-6V
2	S_2, D_1, D_3, D_4, H1,H2	12V	2	S_2, D_1, D_3, D_4, H3,H4	-12V
3	S_1, S_2, D_3, D_4, H1,H2	18V	3	S_1, S_2, D_3, D_4, H3,H4	-18V
4	S_3, D_1, D_2, D_4, H1,H2	24V	4	S_3, D_1, D_2, D_4, H3,H4	-24V
5	S_1, S_3, D_2, D_4, H1,H2	30V	5	S_1, S_3, D_2, D_4, H3,H4	-30V
6	S_2, S_3, D_1, D_4, H1,H2	36V	6	S_2, S_3, D_1, D_4, H3,H4	-36V
7	S_1, S_2, S_3, D_4, H1,H2	42V	7	S_1, S_2, S_3, D_4, H3,H4	-42V
8	S_4, D_1, D_2, D_3, H1,H2	48V	8	S_4, D_1, D_2, D_3, H3,H4	-48V
9	S_1, S_4, D_2, D_3, H1,H2	54V	9	S_1, S_4, D_2, D_3, H3,H4	-54V
10	S_2, S_4, D_1, D_3, H1,H2	60V	10	S_2, S_4, D_1, D_3, H3,H4	-60V
11	S_1, S_2, S_4, D_3, H1,H2	66V	11	S_1, S_2, S_4, D_3, H3,H4	-66V
12	S_3, S_4, D_1, D_2, H1,H2	72V	12	S_3, S_4, D_1, D_2, H3,H4	-72V
13	S_1, S_3, S_4, D_2, H1,H2	78V	13	S_1, S_3, S_4, D_2, H3,H4	-78V
14	S_2, S_3, S_4, D_1, H1,H2	84V	14	S_2, S_3, S_4, D_1, H3,H4	-84V
15	S_1, S_2, S_3, S_4, H1,H2	90V	15	S_1, S_2, S_3, S_4, H3,H4	-90V

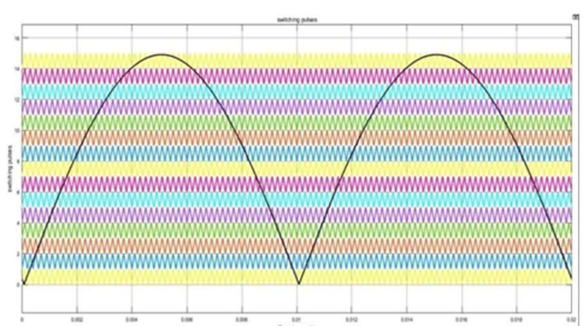

Fig..8 UPD MC for 31-level inverter

It is used to generate switching pulses for semiconductor switches. The modulation index is also very important for generating the optimum output voltage level. The modulation index can change the output voltage and % THD. The formula below may be used to compute the PD modulation index.

$$Ma = \frac{2Am}{(L-1)Ac} = \frac{14.9}{15} = 0.9933 \qquad (12)$$

The reference signal amplitude is represented by 'Am,' while the carrier signal amplitude is represented by 'Ac.' The Modulation Index (MI) 0.993 is used to change the output voltage levels of the proposed architecture. The carriers in the Unipolar Phase Disposition Multicarrier Pulse Width Modulation (UPD MC PWM) method are all in-phase and have the same amplitude and frequency. Figure 9 depicts the carrier layout for the UPD MC PWM method. Positive carriers are plainly seen as operating above the zero-reference axis. A Boolean signal is produced when the unipolar signal (reference) constantly equals to the tri-angular signal. The Boolean signal is then mixed with the logic gates that form the PWM signal for the relevant switches of the proposed MLImaking the use of switching table 3. Calculate the frequency modulation index using the formula below.

$$Mf = \frac{fc}{fr} = \frac{10000}{50} = 200 \text{ ....}(13)$$

The modulation frequency index mf, the carrier switching frequency fc, and the modulating signal frequency fr are all defined here. For the decreased MLI switch, the carrier switching frequency of the multilayer inverter is 10 kHz, and the modulation frequency index is 200.

GRID SYNCHRONIZATION TECHNIQUE USING PI,FUZZY AND ANNCONTROLLERS

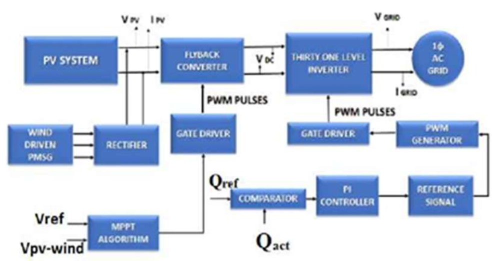

Fig..10. block diagram for grid synchronization

Figure 10 depicts the block diagram grid synchronization of the 31 level ASCHBMLI. The UPD MC PWM inverter determines the PWM switching pattern through the PI, FUZZY, and ANN controllers. The PI, FUZZY, and ANN controllers correct and match the reactive power delivered into the grid (Qact) to its reference (Qref), resulting in a reactive power error. The PI, Fuzzy, and ANN controllers depicted in Fig. below transmit this error through. Establishing a reference angle (#11, 12, 13, and 14). The angle (2) is multiplied by voltage modulation or Vref=14.9V reference voltage and added to grid voltage phase angle sin (1+2). The instantaneous value of the inverter output voltage is determined by comparing the modulating signal with the carrier signal (V). Before the inverter output is linked to the grid, the inverter output voltage and phase must be matched to the grid voltage signal. The main advantage of this control approach is that the reactive power relationship is zero, and the power factor reaches unity.

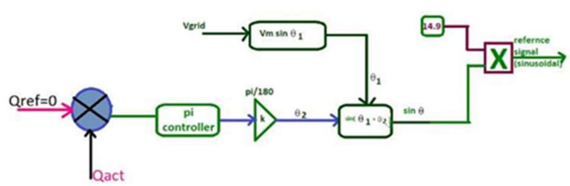

Fig..11 Grid Synchronization Technique Using PI Controller with Fuzzy Controlled MPPT

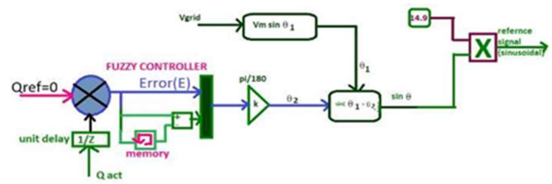

Fig. 12 Grid Synchronization Technique Using Fuzzy Logic Controller with Fuzzy Controlled MPPT

ANN controllers examine the most prevalent approach, the Back-Propagation algorithm, which is a supervised learning, as shown in Figure.13. The Back-Propagation algorithm is based on the steepest-descent approach of error correction. Error-based learning is the most difficult way of descent. It estimates error in connection to an external signal
(i.e., target output) by comparing the target output with calculated output. On the basis of the error signal, the neural network's topology, which includes synaptic connections, that is, the weight matrices, may be changed. It should try to enter a state that produces the fewest possible errors.

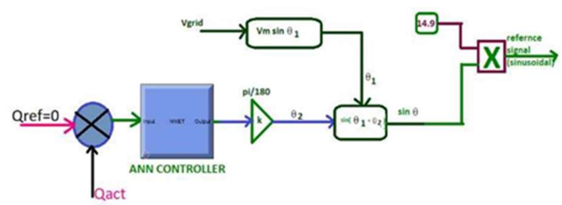

Fig..13 Grid Synchronization Technique Using Ann Controller with Fuzzy Controlled MPPT

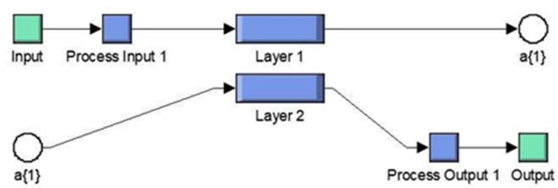

Fig..14 Grid Synchronization Technique Using ANN Controller with two layers.

One input neuron, two hidden layers (minimal error is acquired by the error value created by the trained value in these layers), and one output neuron value are shown in Figure.14.

V. RESULTS

MATLAB verifies the efficiency of the grid-connected renewable hybrid system and conducts practical research with the DSPIC30F2010 controller. The output voltage of the hybrid energy device incorporates higher order ripples due to changes in temperature, irradiation, and wind speed. The recommended converters and inverter reduce such ripples, resulting in a pure sinusoidal wave being sent to the grid via a multilayer inverter. The proposed FLC has a rapid reaction time, low error, high gain, and high efficiency. The voltage was separated into four unsymmetrical dc voltages: 6V, 12V, 24V, and 48V by the multi-tapped transformer.

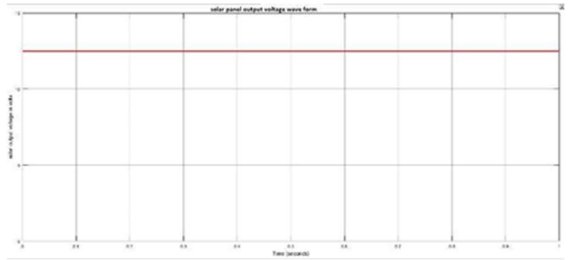

Fig..10 Simulation result of PV panel output voltage waveform

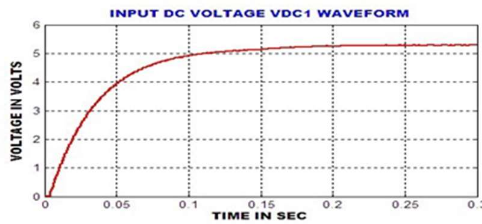

Fig..12 (a) Simulation result of first DC voltage

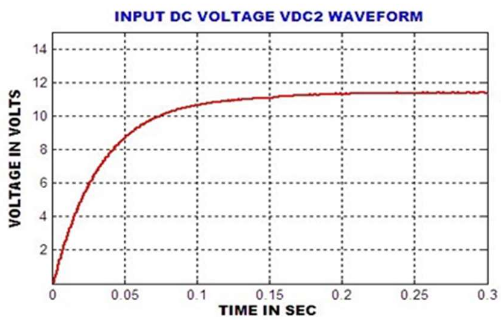

Fig..12) b Simulation result of second DC voltage to the multilevel inverter

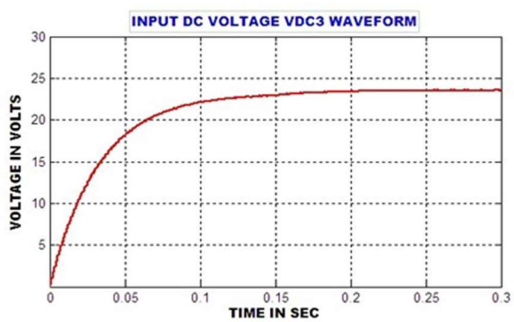

Fig..12(c) Simulation result of third DC voltage

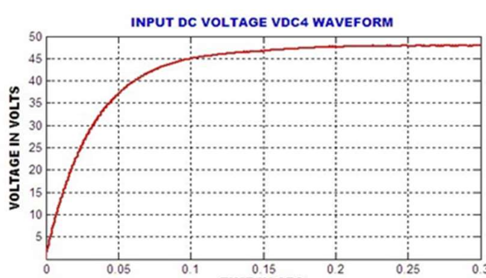

Fig.12 .(d) Simulation output of fourth DC voltage

Fig.13. (a) flyback converter output voltage Vdc1

Fig.13. (b) flyback converter output voltage Vdc2

Fig 13(c) flyback converter output voltage Vdc3

Fig 13(d) flyback converter output voltage Vdc4

The eight unipolar switches in the 31-level ASCHBMLI arrangement create the 31-level output voltage level with a total harmonic distortion of 2.15 percent without employing any filters. The harmonic norm of IEEE 519 is met in terms of percent total harmonic distortion (THD).

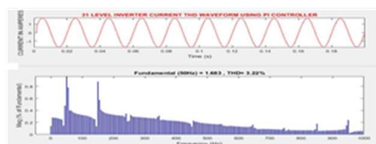

Fig 16 31 level inverter current THD waveform using pi controller with fuzzy logic controlled MPPT

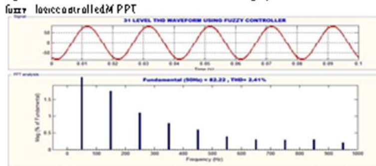

Fig 17 31 level inverter voltage THD waveform using fuzzy logic controller with fuzzy logic controlled MPPT

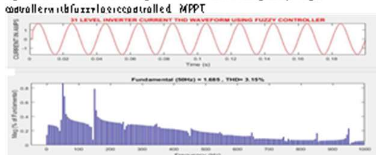

. Fig.18 31 level inverter current THD waveform using fuzzy logic controller

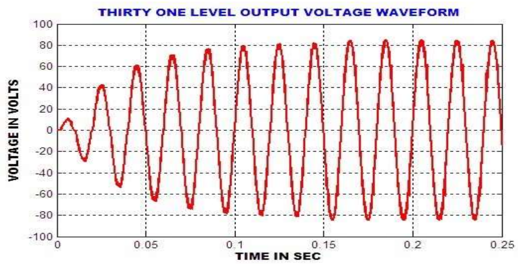

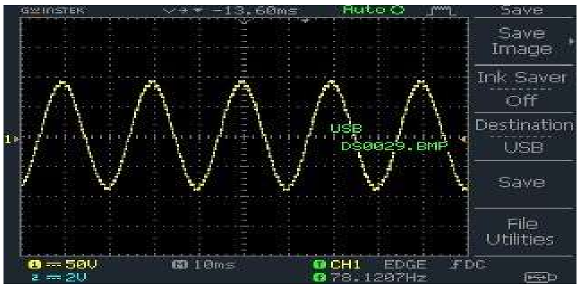

Fig..9(a)and(b)Thirtyonelevelinverteroutputvoltagewaveforms

withfuzzylogic controlled MPPT

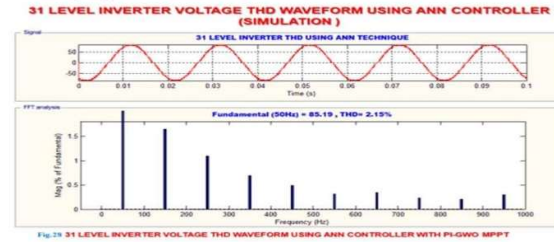

Fig..1931 levelinvertervoltageTHD waveformusingANNcontroller withfuzzylogic controlled MPPT

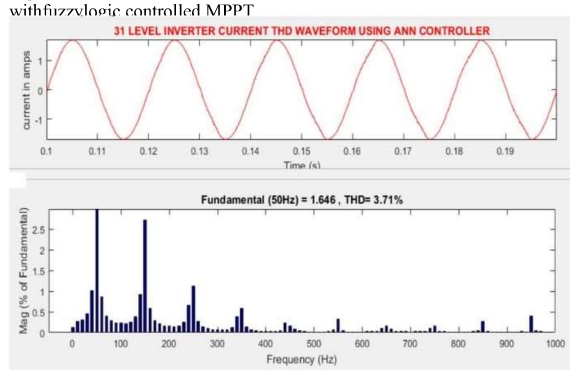

Fig.2031 levelinvertercurrentTHDwaveformusingANN controller with fuzzy logiccontrolledMPPT

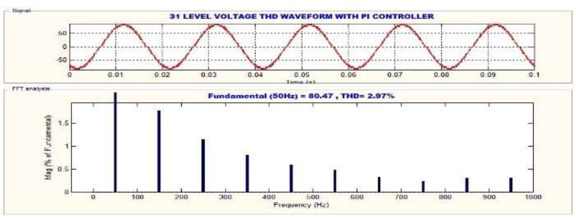

Fig..15 31 level inverter voltage THD waveform using pi controller with fuzzy logic controlled MPPT

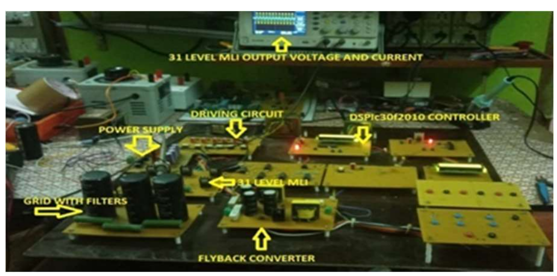

Fig. 21 Thirty-one level inverter Experimental setup

TABLE 4 SHOWS COMPARATIVE ANALYSIS FOR CURRENT AND VOLTAGE THD VALUES FOR DIFFERENT CONTROLLER

S.NO	TECHNIQUE	CURRENT THD	VOLTAGE THD
1	FUZZY MPPT + PI BASED GRID SYNCHRONIZATION	3.22	2.97
2	FUZZY MPPT + FUZZY BASED GRID SYNCHRONIZATION	3.15	2.41
3	FUZZY MPPT + ANN BASED GRID SYNCHRONIZATION	3.7	2.15

Furthermore, Table 2 shows that the proposed flyback converter based on Fuzzy logic controller MPPT with reduced switch MLI with ANN grid synchronization controller outperforms the other methods in Table 4. A digital multi carrier PWM algorithm with PI, Fuzzy, and ANN controllers is implemented in a MATLAB simulation, and the proposed scheme is evaluated with an experimental arrangement using the DSPIC30F2010 Controller.

VI. CONCLUSIONS

The proposed MPPTbased FLC is more popular due to its response faster, errorlow, high gain, and excellent performance. Inverter's efficiencyassessed utilizing the output of converter using PI, FL & ANN controllers. The suggested method's efficiency is confirmed by analyzing the converter output, the MLI output voltage, and the grid THD calculation, respectively. Furthermore, the comparison analysis shows that the proposed FLC-MPPT converter with ANN grid synchronization controlleralong with decreased switches,multi-level inverter outperforms the many alternatives. Lastly,this suggested device is tested with a prototype utilizing the DSPIC30F2010 microcontroller to ensure that the converter and inverter function as expected.

REFERENCES

[1] Soumya. Prabaharan, V. Arun, T. Chinnadurai, K. Arulkumar, A. R. A. Jerin, andK. Palanisamy, ‘‘Analysis of symmetric multilevel inverter using unipolarpulse width modulation for photovoltaic application,’’ComptesRendusl’AcadémieBulgare Sci., vol. 71, no. 2, pp. 252–260, 2018

[2] A. Ramesh, H. HabeebullahSait. "An approach towards selective harmonic elimination switching pattern of cascade switched capacitor twenty-nine-level inverter using artificial bee colony algorithm", Microprocessors and Microsystems, 2020.

[3] J. Gowri Shankar, J. Belwin Edward, K. Sathish Kumar, I. JaocbRaglend. "A 31-level asymmetrical cascaded multilevel inverter with DC-DC flyback converter for photovoltaic system" , 2017 International Conference on High Voltage Engineering and Power Systems (ICHVEPS), 2017.

[4] R. Hemalatha, M Ramasamy. "Microprocessor and PI controller based three phase CHBMLI based DSTATCOM for THD mitigation using 5 1% 6 1% 7 1% 8 1% 9 1% 10 1% 11 hybrid control techniques", Microprocessors and Microsystems, 2020

[5] Mr. GADDALA JAYARAJU and Dr. GUDAPATI SAMBASIVA

RAO,” 31-Level Asymmetrical Cascaded Multilevel Inverter with DCDC Flyback converter for hybrid power distribution” Journal of Information and Computational Science, pp: 115-125, ISSN 1548 – 7741, volume no13, 09-2020.

[6] Gaddala, Jaya Raju and Sambasiva Rao Gudapati. “Unified Power Flow Controller for Non-Linear Loads Using Adaptive Power Quality Theory.” International Journal of Electrical and Computer Engineering 9 (2018): 61-67..

[7] ManyuanYe , Wei Ren, Le Chen, Qiwen Wei, Guizhi Song, And Song Li 2019, ‘Research on Power-Balance Control Strategy of CHB Multilevel Inverter Based on TPWM’, IEEE Access, Vol. 7, 157226 – 157240 ,2017 .

[8] J.Gowri Shankar,.J.Belwin Edward, K.Sathish Kumar and .JaocbRaglend , ‘A 31-Level Asymmetrical Cascaded Multilevel Inverter with DC-DC Flyback converter for Photovoltaic System, 2017 International Conference on High Voltage Engineering and Power System October 2-5, 2017, Bali, Indonesia.

[9] Muralidhar Nayak Bhukya, Venkata Reddy Kota, Shobha Rani Depuru. "A Simple, Efficient, and Novel Standalone Photovoltaic Inverter Configuration with Reduced Harmonic Distortion", IEEE Access, 2019

[10] Mustafa EnginBasoglu& Bekir Cakir , ‘Hybrid global maximum power point tracking approach for photovoltaic power optimizers’, IET Renewable Power Generation, vol.12 no. 8, pp. 875-882,2018.

[11] Chih-Chiang Hua, Yi-Hsiung Fang &Cyuan-Jyun Wong, ‘Improved solar system with maximum power point tracking’, IET Renewable Power Generation, vol.12 no.7, pp. 806-814,2018.

[12] R Girish Ganesan, Mahadevan Bhaskar, K Narayanan. "Novel 11-level Multi-level Inverter", 2018 IEEE Innovative Smart Grid Technologies - Asia (ISGT Asia), 2018

[13] Satyajit Mohanty, BidyadharSubudhi, &Pravat Kumar Ray, ‘A Grey Wolf Assisted Perturb & Observe MPPT Algorithm for a PV System’, Transactions on Energy Conversion, pp. 1-8.

[14] SubhrajyotiModak, Goutam Kumar Panda, Pradip Kumar Saha, ‘Comparative Study between PID-controller and Fuzzy Logic Controller of a Novel Flyback Converter’, International Journal of Advanced Research in Electrical,Electronics and Instrumentation Engineering, vol.4, no.5, pp. 4540-4548,2015

[15] Ashok Kumar L, Indragandhi V & Sujith Kumar N, ‘Design and Implementation of Single-Phase Inverter without transformer for PV
Applications’, IET Renewable Power Generation, vol. 12, no. 5, pp. 547-554, 2018.

[16] Chettibi, N, Mellit, A 2014, ‘FPGA-Based Real Time Simulation and Control of Grid-Connected Photovoltaic Systems’, Science Direct, Simulation Modeling Practice and Theory, vol. 43, pp. 34-53.

[17] DorinPetreus, Stefan Daraban, Ionut Ciocan, Toma Patarau, Cristina
Morel & Mohamed Machmoum 2013, ‘Low-cost Single stage MicroInverter with MPPT for Grid Connected Applications’, SciVerse Science Direct, Solar Energy, vol. 92, pp. 241-255,2013

[18] Dong Cao, Shuai Jiang, Xianhao Yu & Fang Zheng Peng, ‘Low-Cost Semi-Z-source Inverter for Single-Phase Photovoltaic Systems’, IEEE

Transactions on Power Electronics, vol. 26, no. 12, pp. 3514-
3523,2011

[19] Samuel Vasconcelos Araujo, Peter Zacharias & Regine Mallwitz, 'Highly Efficient Single-Phase Transformerless Inverters for GridConnected Photovoltaic Systems', IEEE Transactions on Industrial Electronics, vol. 57, no. 9, pp. 3118-3128,2010.

[20] Kennedy AdinboAganah, Cristopher Luciano, MandoyeNdoye& Gregory Murphy, 'New Switched-Dual-Source Multilevel Inverter for Symmetrical and Asymmetrical Operation', Energies, vol. 11, pp. 0113,2018.

[21] Prabaharan, N., &Palanisamy, K. (2016). A Single-Phase Grid Connected Hybrid Multilevel Inverter for Interfacing Photo-voltaic System. In Energy Procedia (Vol. 103, pp. 250–255).

[22] N. Prabaharan, S. Saravanan, A. R. A. Jerin and K. Palanisamy, "A reduced switch asymmetric multilevel inverter topology using unipolar pulse width modulation strategies for photovoltaic application" in Recent Developments on Power Inverters, Rijeka, Croatia:InTech, pp. 29-48, 2017.

[23] Mr. GADDALA JAYARAJU and Dr. GUDAPATI SAMBASIVA RAO, "Intelligent Controller based Micro-grid Integration of Hybrid PV/Wind and Battery Management System", Journal of Advanced Research in Dynamical and Control Systems, ISSN: 1943-023X, 15Special Issue, 192-201, November-2018.

[24]]G. Jayaraju, G.S. Rao, A new optimized ANN algorithm based single phase grid connected PV-wind system using single switch high gain DC-DC converter, Eur. J. Electr. Eng. 21 (4) (2019) 373–381.

[25] V. Geetha, R. Meenadevi, A 15 Level Multilevel Inverter with Reduced Number of Switches, International Journal of Pure and Applied Mathematics, 119 (2018) 1745-1751.

[26] T. A. Meynard, M. Fadel, N. Aouda, Modeling of Multilevel Converters, IEEE transactions on industrial electronics, 44 (1997) 356364.

[27] K. K. Gupta, S. Jain, Topology for Multilevel Inverters to Attain Maximum Number of Levels from Given DC Sources, IET Power Electronics, 5 (2012) 435-446.

[28] C. K. Lee, S. R. Hui, H. S. H. Chung, A 31-Level Cascade Inverter for Power Applications, IEEE Transactions on Industrial Electronics, 49 (2002) 613-617.

[29] E. Babaei, A Cascade Multilevel Converter Topology with Reduced Number of Switches, IEEE Transactions on Power Electronics, 23 (2008) 2657-2664.

[30] C. Dhanamjayulu, G. Arunkumar, B. Jaganatha Pandian, C. V. Ravi Kumar, M. Praveen Kumar, A. Rini Ann Jerin, P. Venugopal, RealTime Implementation of a 31- Level Asymmetrical Cascaded Multilevel Inverter for Dynamic Loads, IEEE Access, 7 (2019) 5125451266.

[31] R. S. Alishah, D. Nazarpour, S. H. Hosseini, M. Sabahi, New Hybrid Structure for Multilevel Inverter with Fewer Number of Components for High-Voltage Levels, IET power electronics, 7 (2014) 96-104.

[32] M. D. Siddique, S. Mekhilef, N. M. Shah, A. Sarwar, A. Iqbal, M. A. Memon, A New Multilevel Inverter Topology with Reduce Switch Count, IEEE Access, 7 (2019) 58584-58594.

[33] S. Mukherjee, S. De, S. Sanyal, S. Das, S. Saha, A 15-level asymmetric H-bridge multilevel inverter using d-SPACE with PDPWM technique, International Journal of Engineering, Science and Technology, 11 (2019) 22-32.

[34] T. Rakesh, V. Madhusudhan, M. Sushama, An Exploration of MLI Topology and Control Techniques, International Electrical Engineering Journal (IEEJ), 7 (2016).

[35] Venkata Rami Reddy K, Gowri Manohar T. "Modelling and investigation of clean power wind energy systems by using UPQC" , International Journal of Energy Research, 2017 S. Rathore, M. K. Kirar, S. K. Bhardwaj, Simulation of cascaded H-bridge multilevel inverter using PD, POD,.

[36] Ali, R. Ben, Et Al. "Energy Management Of A Small-Scale Wind Turbine System Combined With Battery Storage System." International Journal Of Mechanical And Production Engineering Research And Development 8.3 (2018): 1167-1178.

[37] Kansara, Bindu U., And Br Parekh. "Life Cycle Cost Benefit Analysis Of Battery For Isolated Hybrid Systems–A New Approach And Comperative Analysis."

[38] Deshpande, Soham G., And N. Bhasme. "Modeling And Simulation Of Microinverter With Flyback Converter For Grid Connected Pv Systems." International Journal Of Electrical And Electronics Engineering Research 7.4 (2017): 71-82.

[39] Nguyen, Khuong Vinh, And Nam Nguyen-Quang. "Design And Simulation Of A Photovoltaic-Based Energy System For Mobile Device Chargers At Public Place." International Journal Of Electrical And Electronics Engineering Research 5.1 (2015): 111-118.

[40] Eashwaramma, N., J. Praveen, And M. Vijayakumar. "Reduced Number Of Power Switches In Multi Level Inverter Using Spwm Technique To Mitigate For Sag And Swell." International Journal Of Applied Engineering Research And Development (Ijaerd) 8.1 (2018): 10.

[41] Kiran, B. Madhu, And Bv Sanker Ram. "Analysis Of Cascaded H-Bridge Multilevel Inverter With Level Shifted Pwm On Induction Motor." International Journal Of Electrical And Electronics Engineering Research (Ijeeer) 5 (2015): 11-32.